silver are obtained in small amounts in lab scale experiments.

- The XRD and FESEM–EDAX studies of the metallic product in the present investigation confirm the presence of gold and silver after aqua leaching of e-waste sample.
- TEM–EDX study analysis shows that leached residue also confirms the presence of gold (Au) and silver (Ag).
- The expenditure for the present study was calculated for 1 kg of e-waste sample. It shows that the total value of gain product gives a gain amount Rs 381 (in Indian currency Rupees) with an expenditure of Rs 105 for performing such small experiments. However, the expenditure as well as consumption of such an experiment will certainly come down in a continuous large scale operation, which makes the process more economical. Moreover, air instead of H_2O_2 as an oxidizing agent; will also cut down the cost further.
- The entire investigation shows that microwave heat treatment is not only a clean process but also an eco-friendly process for obtaining valuable precious metals like gold and silver metals from e-waste.

1. Khanna, R., Cayumil, R., Mukherjee, P. S. and Sahajwalla, V., A novel recycling approach for transforming waste printed circuit boards into a material resource. *Proc. Environ. Sci.*, 2014, **21**, 42–54.
2. Cui, J. and Zhanga, L., Metallurgical recovery of metals from electronic waste: a review. *J. Hazard. Mater.*, 2008, **158**, 228–256.
3. Dey, S. and Jana, T., E-waste recycling technology patents filed in India – an analysis. *J. Intell. Prop. Rights*, 2014, **19**, 315–324.
4. Buekens, Alfons and Jie, Y., Recycling of WEEE plastics: a review. *J. Mater. Cycles Waste*, 2014, **16**, 415–434.
5. Balde, K., The Global E-waste Monitor 2014 – Quantities, flows and resources. United Nation University; https://i.unu.edu/media/unu.edu/news/52624/UNU-1stGlobal-E-Waste-Monitor-2014-small.pdf
6. Pant, D., Joshi, D., Manoj Upreti, K. and Ravindra, K. K., Chemical and biological extraction of metals present in e-waste: a hybrid technology. *Waste Manage.*, 2012, **32**, 979–990.
7. Chaurasia, A., Singh, K. K. and Mankhand, T. R., Extraction of tin and copper by acid leaching of PCBs. *Int. J. Metall. Eng.*, 2013, **2**(2), 243–248.
8. Bala, I. A. K. and Hassan, M. A. A., Thermal plasma treatment of wastes: a review. *Aust. J. Basic Appl. Sci.*, 2015, **9**(31), 322–333.
9. Biswajit, R., Thermal plasma treatment of mobile phone waste under reduced condition. *Int. J. Environ. Sci.*, 2012, **2**(4), 1–8.
10. Cerqueira, N., Vandensteendam, C., Baronnet, J. M. and Girold, C., Heavy metals volatility during thermal plasma vitrification of mineral waste. *Environ. Eng. Sci.*, 2004, **21**(1), 83–92.
11. Abdul, K., Rhamdhani, M. A., Brooks, G. and Syed, M., Metal extraction processes for electronic waste and existing industrial routes: a review and Australian perspective. *Resources*, 2014, **3**, 152–179.
12. Cheng, T. W., Chu, J. P., Tzeng, C. C. and Chen, Y. S., Treatment and recycling of incinerated ash using thermal plasma technology. *Waste Manage.*, **22**(5), 485–490.
13. Srikant, S. S., Mukherjee, P. S. and Rao, R. B., Morphological characterization of titania slag obtained from red sediment placer ilmenite using microwave energy. *J. Inst. Eng. India Ser. D*, 2015, **96**, 43–49.
14. Srikant, S. S., Mukherjee, P. S. and Rao, R. B., Prospects of microwave energy in material and mineral processing. *Turk. J. Eng. Sci. Technol.*, 2013, **2**, 23–31.
15. Pickles, C. A., Microwaves in extractive metallurgy: Part 1 – A review of fundamental. *Miner. Eng.*, 2009, **22**, 1102–1111
16. Srikant, S. S., Mukherjee, P. S. and Rao, R. B., Microwave energy for waste management. *Mineral Process. Technol.*, 2013, **3**, 948–953.
17. Srikant, S. S., Mahapatra, R. P. and Laxmi, T., Microwave energy for waste used engine oil. *The Institution of Engineers (India) Odisha State J.*, 2015, **1**, 255–261.

Anti-inflammatory activity of synthesized diarylpentenedione derivatives and their drug delivery with silicon-nanotube (7,7)

A. Surendar[1], S. K. Sadulla[1], Ali Noory Fajer[2], Mazhar Abbas[3] and Meysam Najafi[4,*]

[1]School of Electronics, Vignan's Foundation for Science, Technology and Research, Guntur 522 213, India
[2]Department of Biology, Education College, University of Al-Qadisiyah, Al Diwaniyah, Qadisiyyah, Iraq
[3]Department of Management Sciences, COMSATS University, Islamabad Vehari Campus, Pakistan
[4]Medical Biology Research Center, Kermanshah University of Medical Sciences, Kermanshah 67149-67346, Iran

Earlier studies have confirmed that diarylpentenedione derivaties 1a and 1c have the highest and the lowest anti-inflammatory activity respectively. In this work, the interactions of diarylpentenedione derivatives 1a–1c with Si-nanotube (7,7) were studied and quantum molecular descriptors of the diarylpentenedione derivatives were calculated. Results showed that 1a–1c can interact with Si-nanotube (7,7) significantly and so their adsorptions were possible from an

*For correspondence. (e-mail: meysamnajafi2016@yahoo.com)

energetic viewpoint. Results also indicated that adsorption thermodynamic values of 1a on Si-nanotube (7,7) were higher than those of 1b and 1c. Therefore 1a has the highest chemical potential and electrophilicity index values. Thus the obtained theoretical and published experimental trends of anti-inflammatory activity of 1a–1c were similar.

Keywords: Adsorption energy, anti-inflammatory and chemical potential, diarylpentenedione derivatives, silicon nanotube.

INFLAMMATION is a defensive answer that it includes the defended cells, blood vessels and molecular arbitrator. The aim of inflammation is start to correction of tissue. Anti-inflammatory mentions to treatment of inflammation in body[1–3]. Diarylpentanoid derivatives are potential anti-inflammatory drugs to remove the monocyte chemoattractant[4–6].

Nanoparticles such as silicon nanotubes have large band gaps and high performance to therapeutic drug delivery[7–11]. In the present work, the interactions of diarylpentenedione derivatives 1a–1c (Figure 1) with Si-nanotube (7,7) were studied (Figure 2) to propose new anti-inflammatory drugs.

The chemical potential ($\mu = (E_{LUMO} + E_{HOMO})/2$), chemical hardness ($\eta = (E_{LUMO} - E_{HOMO})/2$) and electrophilicity index ($\omega = \mu^2/2\eta$) as quantum molecular descriptors can establish the chemical potential of various drugs. The μ expresses the constancy of drug in contradiction of electronic configuration variations. η characterizes the energy gap of a drug, and therefore drugs with lower η values are more reactive. ω measures the ability of a drug to accept electrons. The interactions between drugs and nanostructures can be examined using the following relation: $\Delta N = (\mu_D - \mu_N)/(2\eta_D + 2\eta_N)$, where μ_D and μ_N are the chemical potential of the drugs, while η_D and η_N are the chemical hardness of the drugs and nanostructures respectively[12–14].

In this study, the μ, η, ω and ΔN values of diarylpentenedione derivatives have been calculated in order to establish the capability of Si-nanotube (7,7) to transmission of diarylpentenedione derivatives 1a–1c. The aim of this work is to: (1) to compare the ΔE_{ad} and ΔG_{ad} values of 1a–1c on the Si-nanotube (7,7) surface; (2) to study the quantum molecular descriptors of 1a–1c and (3) to also study the anti-inflammatory activity of 1a–1c.

In this study, the geometries of Si-nanotube (7,7), diarylpentenedione derivatives 1a–1c and their complexes with Si-nanotube (7,7) via 6-31G(d) basis set and density functional theory method in GAMESS package were optimized[15–18]. The interaction values of 1a–1c and Si-nanotube (7,7) were calculated as

$$\Delta E_{ad} = E\,(\text{Si-nanotube }(7,7)/\text{drug}) - E\,(\text{drug})$$
$$- E\,(\text{Si-nanotube }(7,7)) + E_{BSSE}, \qquad (1)$$

$$\Delta G_{ad} = G\,(\text{Si-nanotube }(7,7)/\text{drug}) - G\,(\text{drug})$$
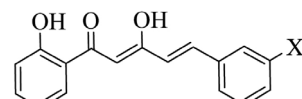$$- G\,(\text{Si-nanotube }(7,7)) + E_{BSSE}. \qquad (2)$$

where E (Si-nanotube (7,7)/drug) corresponds to the energy of complexes of 1a–1c with Si-nanotube (7,7); and E (Si-nanotube (7,7)) and E (drug) correspond to energy of 1a–1c and Si-nanotube (7,7) respectively; G (Si-nanotube (7,7)/drug) corresponds to the free Gibbs energy of complexes of 1a–1c with Si-nanotube (7,7) and G (Si-nanotube (7,7), and G (drug) correspond to the free Gibbs energy of 1a–1c and Si-nanotube (7,7) respectively. E_{BSSE} is the basis set superposition error energy by counterpoise modification method. Negative values of ΔE_{ad} and ΔG_{ad} correspond to exothermic adsorption of 1a–1c on the surface of Si-nanotube (7,7) (ref. 19).

Leong et al.[20] synthesized a chain of diarylpentenedione derivatives (1a–1c) and examined their anti-inflammatory activity against RAW 264.7 cell using experimental methods (Figure 1). They showed that diarylpentenedione derivative 1a has the highest action against RAW 264.7 cell, while diarylpentenedione derivative 1c has the highest IC$_{50}$ value and the lowest action against RAW 264.7 cell[20]. Thus the anti-inflammatory activity of these diarylpentenedione derivatives can be represented as follows: 1c < 1b < 1a.

Leopoldini et al.[21] examined the theoretical parameters of several phenolic drugs using the DFT/B3LYP method. Nam et al.[22] studied the theoretical parameters for pyridinethiol derivatives using the DFT/B3LYP method, while Mohajeri and Asemani[23] examined those of chroman derivatives using DFT method.
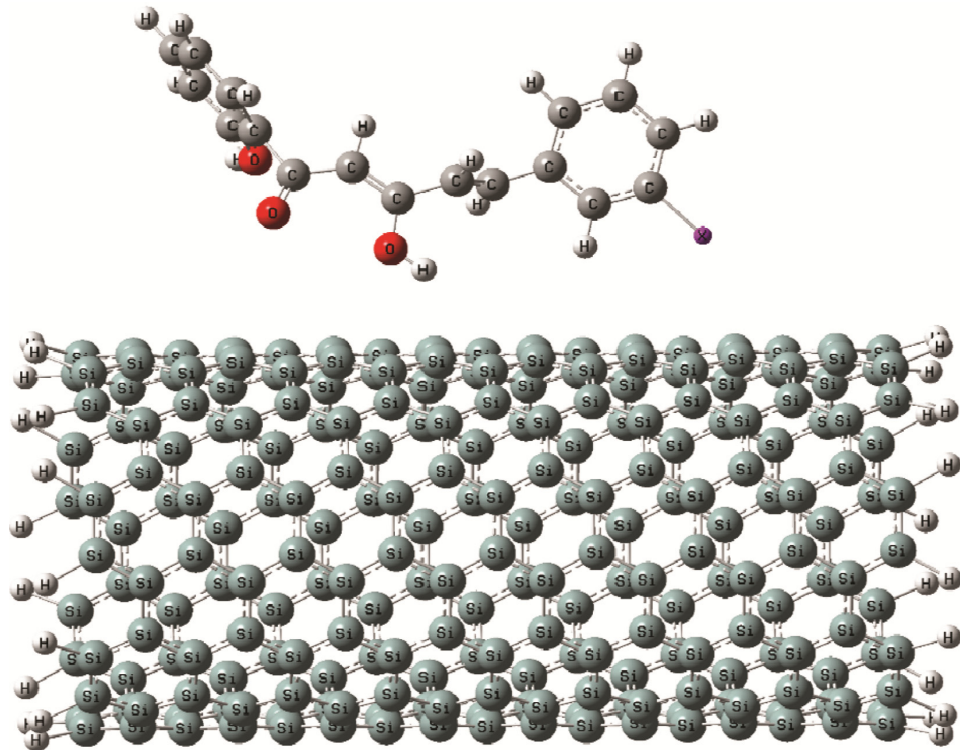
Researchers[21–23] showed that DFT/B3LYP method can calculate the experimental activity of drugs, significantly. Rimarcik et al.[24] studied the activity of several anilines using the B3LYP method. Brinck et al.[25] calculated the activity of the drugs via DFT/B3LYP and 6-31G(d, p) basis set. They confirmed there are linear dependencies between the experimental and theoretical activities of studied drugs.

Klein and co-workers[26–28] confirmed using the theoretical and experimental methods that antioxidant activity

Derivative	X	Nitric oxid inhibition
1a	Cl	26.7
1b	Br	29.4
1c	OMe	31.6

Figure 1. Structures of diarylpentenedione derivatives 1a–1c and published IC$_{50}$ values (in μM) against RAW 264.7 cell in previous literature[20].

Figure 2. Interactions of diarylpentenedione derivatives **1a–1c** with Si-nanotube (7,7).

of drugs such as chromans has linear dependencies. Kumar *et al.*[29] studied the properties of naturally occurring flavonoids such as chrysoeriol and hispidulin using DFT/B3LYP.

Sadasivam and Kumaresan[30] reported that antioxidant activity of drugs via theoretical method (DFT/B3LYP) and experimental scales have same trends. Therefore, it can be concluded that the DFT/B3LP method can predicate the experimental properties of various drugs and also propose novel drugs with high activity[21–30].

In the present study, the ΔE_{ad} and ΔG_{ad} values of **1a–1c** on Si-nanotube (7,7) surface were calculated. Table 1 shows the ΔE_{ad} values of **1a** and **1b** on Si-nanotube (7,7) are higher than that of **1c**. Also, the ΔE_{ad} value of **1a** on Si-nanotube (7,7) is higher than that of **1b**.

The ΔG_{ad} value of **1a** on Si-nanotube (7,7) is higher than those of **1b** and **1c** Also, the ΔG_{ad} value of **1b** on Si-nanotube (7,7) is higher than that of **1c**. ΔG_{ad} values of **1a–1c** on Si-nanotube (7,7) are lower than ΔE_{ad}. Thus the results show that ΔE_{ad} and ΔG_{ad} values of **1a–1c** on Si-nanotube (7,7) surface are negative and decrease as follows: **1c** < **1b** < **1a**. Adsorption of **1a–1c** on Si-nanotube (7,7) surface is possible from the thermodynamic viewpoint. The diarylpentenedione derivatives **1a** and **1c** have the highest and the lowest probable to Si-nanotube (7,7) respectively.

The diarylpentenedione derivatives (**1a–1c**) as phenolic structures can play a protective role via three mechanisms. In the first one, the free radical removes a hydrogen atom from **1a–1c**. In the second, the diarylpentenedione derivatives can donate an electron to the free radical and drug become a radical cation. In the third, drugs **1a–1c** can transfer protons to the free radical and they become anion structures. The bond dissociation enthalpy (BDE), ionization potential (IP) and proton affinity (PA) are important parameters that provide information about the efficiency of the diarylpentenedione derivatives activity. The lower BDE, IP and PA values of **1a–1c** increase the reaction of free radical inactivation and electron abstraction[20–30].

In this study, BDE, IP and PA of **1a–1c** were indicated using 6-31G(d) basis set and density functional theory method.

The BDE values of **1a–1c** were calculated via differences in enthalpies of diarylpentenedione, hydrogen atom and diarylpentenedione in radical form as follows

BDE = H (diarylpentenedione in radical form)

– H (diarylpentenedione) – H (hydrogen atom).

The IP values of **1a–1c** were calculated via differences of enthalpies in diarylpentenedione, electron and diarylpentenedione in cation radical form as follows

IP = H (diarylpentenedione in cation radical form)

– H (diarylpentenedione) – H (electron).

The PA values of **1a**–**1c** were calculated via differences enthalpies of diarylpentenedione, proton and diarylpentenedione in anion form as follows

PA = H (diarylpentenedione in anion form)

    – H (diarylpentenedione) – H (proton).

Table 1 shows the calculated BDE, IP and PA values of **1a**–**1c**. The calculated BDE values of **1a**–**1c** decreased as follows: **1a** < **1b** < **1c**. Thus, **1a** has the highest capacity and **1c** has the lowest capacity to lose hydrogen atom.

The calculated IP values of **1a**–**1c** decreased as follows: **1a** < **1b** < **1c**. Thus **1a** has the highest capacity and **1c** has the lowest capacity to lose an electron.

The calculated PA values of **1a**–**1c** decreased as follows: **1a** < **1b** < **1c**. Thus **1a** has the highest capacity and **1c** has the lowest capacity to lose a proton.

Table 2 shows the calculated μ, η and ω values of **1a**–**1c** and Si-nanotube (7,7). The calculated μ values of **1a**–**1c** decreased as follows: **1a** > **1b** > **1c**. Thus **1a** has the highest and **1c** has the lowest capacity to accept an electron. The calculated η values show that **1a** has the lowest stability and the highest reactivity and **1c** has the lowest reactivity.

The calculated ω values of **1a**–**1c** decreased as follows: **1a** > **1b** > **1c**. Thus **1a** has the highest and **1c** has the lowest capacity to accept electrons.

Table 2 also shows the calculated ΔN values of complexes of **1a**–**1c** with Si-nanotube (7,7). The diarylpentenedione derivatives **1a**–**1c** act as electron donors and boron nitride-nanotube (9,9) acts as an electron acceptor. Also, **1a** has the highest ΔN value and the highest interactions with Si-nanotube (7,7).

Thus the anti-inflammatory activity of diarylpentenedione derivatives was found to decrease as follows: **1c** < **1b** < **1a**. The adsorption potential of **1a**–**1c** decreased as follows: **1a** > **1b** > **1c**. Calculations show that

1a has the highest value and **1c** has the lowest μ and ω values. It can be concluded that the calculated μ, η, ω values of **1a**–**1c** and their ΔE_{ad} and ΔG_{ad} values have similar trends. These theoretical trends confirm the experimental trends of anti-inflammatory activity of **1a**–**1c**. The ΔE_{ad}, ΔG_{ad}, μ, η and ω values derivatives **1a**–**1c** are vital parameters to predicate their adsorption potential on the Si-nanotube (7,7) surface.

In this study, the anti-inflammatory activity of diarylpentenedione derivatives **1a**–**1c** were examined using theoretical methods and the obtained results were compared with the reported experimental results[20]. Experimental results showed that **1a** and **1c** have the highest and lowest anti-inflammatory activity respectively. The interactions of **1a**–**1c** with Si-nanotube (7,7) were examined and the quantum molecular descriptors of the diarylpentenedione derivatives were calculated. The adsorption parameters (ΔE_{ad} and ΔG_{ad}) of **1a**–**1c** on Si-nanotube (7,7) surface were studied using density functional theory method. Results show that, **1a**–**1c** can interact with Si-nanotube (7,7) significantly and their adsorption on Si-nanotube (7,7) surface is possible from a thermodynamic viewpoint. The adsorption ability of the diarylpentenedione derivatives decreased as follows: **1a** > **1b** > **1c** and **1a**. Also, **1a** has the highest and **1c** the lowest potential for adsorption on Si-nanotube (7,7). In addition, **1a** has the highest μ and ω values and the lowest η value. Results indicated that theoretical and experimental trends of activity of diarylpentenedione derivatives **1a**–**1c** are similar.

1. Blagg, J., Structure-activity relationships for *in vitro* and *in vivo* toxicity. *Annu. Rep. Med. Chem.*, 2006, **41**, 353–368.
2. Razavi, R., Hosseini, S. M. A. and Ranjbar, M., Production of nanosized synthetic rutile from ilmenite concentrate by sonochemical HCl and H_2SO_4 leaching. *Iran. J. Chem. Chem. Eng.*, 2014, **33**, 29–36.
3. Razavi, R., Kardani, M. N., Ghanbari, A., Lariche, M. J. and Baghban, A., Utilization of LSSVM algorithm for estimating synthetic natural gas density. *Petrol. Sci. Technol.*, 2018, **36**, 807–812.
4. Parsaee, Z., Karachi, N. and Razavi, R., Ultrasound assisted fabrication of a novel optode base on a triazine based Schiff base immobilized on TEOS for copper detection. *Ultrason. Sonochem.*, 2018, **47**, 36-46.
5. Zahedifar, M., Razavi, R. and Sheibani, H., Reaction of (chloro carbonyl) phenyl ketene with 5-amino pyrazolones: Synthesis, characterization and theoretical studies of 7-hydroxy-6-phenyl-3-(phenyldiazenyl) pyrazolo[1,5-a]pyrimidine-2,5(1H,4H)-dione derivatives. *J. Mol. Struct.*, 2016, **1125**, 730–735.
6. Karachi, N., Hosseini, M., Parsaee, Z. and Razavi, R., Novel high performance reduced graphene oxide based nanocatalyst decorated with Rh_2O_3/Rh-NPs for CO_2 photoreduction. *J. Photochem. Photobiol. A. Chem.*, 2018, **364**, 344–354.
7. Seyedi, S. H., Saray, B. N. and Nobari, M. R. H., Using interpolation scaling functions based on Galerkin method for solving non-Newtonian fluid flow between two vertical flat plates. *Appl. Math. Comput.*, 2015, **269**, 488–496.
8. Moraga, R. J. and Rabiei Hosseinabad, E., A system dynamics approach in air pollution mitigation of metropolitan areas with sustainable development perspective: a case study of Mexico City. *J. Appl. Environ. Biol. Sci.*, 2017, **7**, 164–174.

Table 1. Calculated ΔE_{ad} and ΔG_{ad} (eV) of diarylpentenedione derivatives **1a**–**1c** on surface of Si-nanotube (7,7). The BDE, IP and PA values (eV) of studied structures

Structures	ΔE_{ad}	ΔG_{ad}	BDE	IP	PA
1a	−0.55	−0.45	11.8	17.3	8.4
1b	−0.41	−0.37	13.2	18.9	9.1
1c	−0.34	−0.26	14.6	20.1	9.9

Table 2. μ, η, ω and ΔN (eV) values **1a**–**1c** and Si-nanotube (7,7)

Structure	μ	η	ω	ΔN
Si-nanotube (7,7)	−0.55	0.10	1.56	–
1a	−0.47	0.07	1.66	−0.250
1b	−0.46	0.11	0.99	−0.225
1c	−0.45	0.14	0.73	−0.217

9. Feili, H. R., Ahmadian, P. and Rabiei, E., Life cycle assessment of municipal solid waste systems to prioritize and compare their methods with multi-criteria decision making. *OAJRE*, 2014, **39**, 1–12.

10. Azhiri, R. B., Sola, J. F., Tekiyeh, R. M., Javidpour, F. and Bideskan, A. S., Analyzing of joint strength, impact energy, and angular distortion of the ABS friction stir welded joints reinforced by nanosilica addition. *Int. J. Adv. Manuf. Technol.*, 2018, **1**, 1–14.

11. Azhiri, R. B., Tekiyeh, R. M., Zeynali, E., Ahmadnia, M. and Javidpour, F., Measurement and evaluation of joint properties in friction stir welding of ABS sheets reinforced by nanosilica addition. *Measurement*, 2018, **127**, 198–204.

12. Ketabchy, M., Sample, D. J., Wynn-Thompson, T. and Yazdi, M. N., Thermal evaluation of urbanization using a hybrid approach. *J. Environ. Manage.*, 2018, **226**, 457–475.

13. Joshaghani, M., Ghasemi-Fare, O. and Ghavami, M., Experimental investigation on the effects of temperature on physical properties of sandy soils. *IFCEE*, 2018, **1**, 675–685.

14. Khodabandeh, E., Rozati, S. A., Joshaghani, M., Akbari, O. A., Akbari, S. and Toghraie, D., Thermal performance improvement in water nanofluid/GNP–SDBS in novel design of double-layer microchannel heat sink with sinusoidal cavities and rectangular ribs. *J. Therm. Anal. Calorim.*, 2018, **1**, 1–13.

15. Jafarzadeh, F., Jahromi, H. F., Yoosefi, S., Sehizadeh, M., Joshaghani, M. and Alavi, M., Dynamic response of buried gas pipelines due to earthquake induced landslides by nonlinear numerical modeling. In The 15th World Conference on Earthquake Engineering, Beijing, China (15WCEE), 2012.

16. Pourmand, G., Safavi, M., Ahmadi, A., Houdeh, E., Noori, M., Mashhadi, R. and Pourmand, N., A silver lining for early diagnosis of prostate cancer. *Urol. J.*, 2016, **13**, 2845–2848.

17. Bakhshi, H., Khodabandeh, E., Akbari, O., Toghraie, D., Joshaghani, M. and Rahbari, A., Investigation of laminar fluid flow and heat transfer of nanofluid in trapezoidal microchannel with different aspect ratios. *Int. J. Numer. Method H.*, 2018, **1**, 1–13.

18. Pirbazari, A. E., Monazzam, P. and Kisomi, B. F., Desalin. Co/TiO₂ nanoparticles: preparation, characterization and its application for photocatalytic degradation of methylene blue. *Water Treat.*, 2017, **63**, 283–292.

19. Ebrahimian Pirbazari, A., Fakhari Kisom, B. and Ghamangiz Khararoodi, M., Anionic surfactant-modified rice straw for removal of methylene blue from aqueous solution. *Desalin. Water Treat.*, 2016, **57**, 18202–18216.

20. Momtazan, M., Niyakan, M., Jaderi, T. and Hoseini Ahangari, S. A., The amount of scientific production of Ahvaz Jundishapur university of medical sciences on pubmed in 2000–2013. *Res. J. Med. Sci.*, 2016, **10**, 49–53.

21. Leopoldini, M., Marino, T., Russo, N. and Toscano, M., Antioxidant properties of phenolic compounds: H-atom versus electron transfer mechanism. *J. Phys. Chem. A*, 2004, **108**, 4916–4922.

22. Nam, P. C., Nguyen, M. T. and Chandra, A. K., Assessment of the importance of changes in ground-state energies on the bond dissociation enthalpies of the O–H bonds in phenols and the S–H bonds in thiophenols. *J. Phys. Chem. A*, 2006, **110**, 10904–10911.

23. Mohajeri, A. and Asemani, S. S., Theoretical investigation on antioxidant activity of vitamins and phenolic acids for designing a novel antioxidant. *J. Mol. Struct: (Theochem)*, 2009, **930**, 15–20.

24. Rimarcik, J., Lukes, V., Klein, E., Griesser, M. and Kelterer, A., Theoretical study of structure and electronic properties of cyano-substituted pyrroles. *Chem. Phys.*, 2008, **353**, 177–184.

25. Brinck, T., Haeberline, M. and Jonsson, M., Theoretical study of X–H bond energetics (X = C, N, O, S) application to substituent effects, gas phase acidities, and redox potentials. *J. Am. Chem. Soc.*, 1997, **119**, 4239–4244.

26. Klein, E. and Lukes, V., Proton Affinities of para- and meta-substituted phenols in water. *Chem. Phys.*, 2006, **330**, 515–525.

27. Najafi, M., Zahedi, M. and Klein, E., DFT/B3LYP study of the solvent effect on the reaction enthalpies of homolytic and heterolytic OH bond cleavage in mono-substituted chromans. *Comput. Theor. Chem.*, 2011, **978**, 16–28.

28. Klein, E., Lukes, V. and Cibulkova, Z., Quantum-chemical study of C–H bond dissociation enthalpies of various small non-aromatic organic molecules. *J. Mol. Struct.: (Theo-chem.)*, 2006, **758**, 149–159.

29. Kumar, D., Kumar, N. M. and Sundaree, S., A facile synthesis of novel bis-(indolyl)-1,3,4-oxadiazoles as potent cytotoxic agents. *Eur. J. Med. Chem.*, 2010, **45**, 1244–1249.

30. Sadasivam, K. and Kumaresan, R., Theoretical investigation on the antioxidant behavior of chrysoeriol and hispidulin flavonoid compounds a DFT study. *Comput. Theor. Chem.*, 2011, **963**, 227–235.

Allocation of biomass and carbon stocks in seven woody species of tropical deciduous forests, Dang, Gujarat

Ekta Purswani[1], Bhawana Pathak[1,*] and Harshad Salvi[2]

[1]School of Environment and Sustainable Development, Central University of Gujarat, Gandhinagar 382 030, India
[2]Gujarat Ecological Education and Research Foundation, Gandhinagar 382 007, India

Literature on the biomass estimates and carbon cycles of Asian tropical deciduous forests is very limited. In this study, seven woody species were selected, with four representatives each in chronosequence, and harvested from deciduous forests of Dang, Gujarat for assessing their biomass and carbon content. All the species showed a carbon percentage between 40% and 45%. The regression equations of total biomass versus girth class developed for all seven species would be useful to estimate biomass on a larger scale and the carbon content would improve the understanding about carbon accounts of Indian forests.

Keywords: Biomass estimation, carbon sequestration, climate change, Indian forests, tropical deciduous forests.

ABOUT 17% of the global CO_2 emissions occur due to deforestation and land-use change[1]. Reduction of emissions through deforestation and forest degradation (REDD+)

*For correspondence. (e-mail: bhawana.pathak@cug.ac.in)